NANO LETTERS

Letter

Role of Semiconducting and Metallic Tubes in P3HT/Carbon-Nanotube Photovoltaic Heterojunctions: Density Functional Theory Calculations

Yosuke Kanai, and Jeffrey C. Grossman

Nano Lett., **2008**, 8 (3), 908-912 • DOI: 10.1021/nl0732777 • Publication Date (Web): 22 February 2008

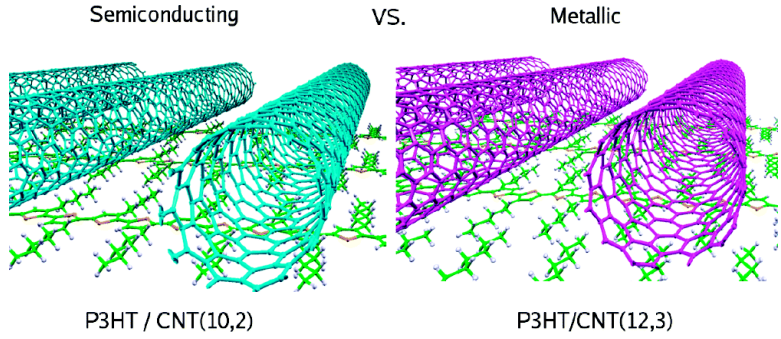

More About This Article

Additional resources and features associated with this article are available within the HTML version:

- Supporting Information
- Links to the 2 articles that cite this article, as of the time of this article download
- Access to high resolution figures
- Links to articles and content related to this article
- Copyright permission to reproduce figures and/or text from this article

View the Full Text HTML

NANO LETTERS

2008
Vol. 8, No. 3
908-912

Role of Semiconducting and Metallic Tubes in P3HT/Carbon-Nanotube Photovoltaic Heterojunctions: Density Functional Theory Calculations

Yosuke Kanai* and Jeffrey C. Grossman

Berkeley Nanosciences and Nanoengineering Institute and Center of Integrated Nanomechanical Systems, University of California, Berkeley, California 94720

Received December 14, 2007; Revised Manuscript Received January 31, 2008

ABSTRACT

A density functional theory approach is employed to investigate poly-3-hexylthiophene (P3HT) interfaced with both a semiconducting and metallic carbon nanotube (CNT). For the semiconducting CNT, a type-II heterojunction can form, making such an interface desirable as a photovoltaic heterojunction. In contrast, with the metallic CNT, substantial charge redistribution occurs and the interaction is strongly enhanœd. The built-in-potential is, however, quite small, and P3HT becomes electrostatically more attractive for electrons. These observations together indicate that, in a photovoltaic heterojunction based on a mixed CNT distribution, the majority of interfaces are with metallic CNTs and inefficient.

Nanomaterials offer exciting possibilities for photovoltaic (PV) applications[1–3] because of the ability to engineer and tailor their optical and electronic properties by controlling the material size, symmetry, and surface while maintaining low cost. One promising class of nano-PV devices is the excitonic solar cell (XSC),[4] although the realization of efficient PV devices based on the XSC concept remains highly challenging. Compared with conventional cells, excitons are more strongly bound in XSCs and must be dissociated at an interface of two different materials in order to produce charge carriers.[5] Therefore, the electronic properties of this nanoscale interface are of fundamental importance for the production of free charge carriers and essential for efficient XSC devices.

One of the most successful XSCs is based on a polymer/fullerene blend.[2] In particular, the ∼5% power conversion efficiency reported[6] for the poly-3-hexylthiophene (P3HT)/fullerene device is quite encouraging, especially given that the P3HT phase absorbs only about 20% of standard AM1.5 solar photons due to the spectral mismatch.[7] The charge-separation process in this PV cell is known to be extremely efficient, leading to an external quantum efficiency over 70%.[8] Charge separation at the heterojunction interface involves the dissociation of an exciton that has diffused from within the polymer to the interface, transferring the electron to the fullerene side while leaving the hole behind in the polymer phase. While efficient electron transfer is clearly beneficial for the PV cell,[9,10] the separated charges must move away from the interface quickly in order to inhibit subsequent charge recombination. The use of carbon nanotubes (CNT) in place of fullerenes is a natural direction for improving the efficiency by incorporating a pre-existing percolation network instead of an assembled network of fullerenes.[11] Additionally, CNT appear to form ideal ohmic contacts with a number of different metal electrodes for the electrons, as in the C_{60} case.[12]

Carbon nanotubes also conveniently provide continuous (semi-infinite) electronic states in the conduction band for accepting the transferring electrons from the π^* state of polythiophenes. According to Fermi's golden rule, the nonadiabatic electron transfer is expected to be highly efficient with the semi-infinite acceptor states in the CNT, as in the case of Dye-TiO_2 nanoparticle systems.[13] In addition, the close spatial proximity and degeneracy of the P3HT π^* state to some of the CNT conduction band states might allow for strong wave function overlap, therefore also leading to an efficient adiabatic mechanism for electron transfer in an excited state. Regardless of the mechanism, an efficient exciton dissociation step can be expected *if* the type-II heterojunction can be formed.

Despite the conceptual advantage of its design, experimental efficiencies of the polythiophene/CNT solar cell remain considerably lower than those of the polymer/fullerene system[14–16] and the mixed chirality distribution with

* Corresponding authors. E-mail: ykanai@berkeley.edu (Y.K.); jgrossman@berkeley.edu (J.C.G.).

10.1021/nl0732777 CCC: $40.75
Published on Web 02/22/2008

semiconducting and metallic CNT makes it difficult to understand the shortcomings and improve the efficiency. Furthermore, the roles of semiconducting and metallic nanotubes for photocurrent generation are at present not well understood. Earlier studies relied on the assumption that the dominant presence of either metallic or small band gap (0.1–0.2 eV) semiconducting tubes provides a sizable built-in potential at the interface for the holes to drift away.[17] However, recent work also recognizes the possibility that the metallic tubes could be the limiting factor because of enhanced electron–hole recombination.[15] In other recent experiments, the CNT Fermi level was suggested to be blue-shifted with respect to the contacting P3HT, resulting in a large built-in potential; this was attributed to ground-state charge-transfer from the polythiophene sulfur atoms to the CNT.[16] Despite these and other experimental studies[18–21] on this important and other related promising polymer/CNT PV systems, little if any theoretical work has been carried out to date. Yet a detailed atomistic picture of the heterojunction electronic structure could provide important insights and shed light on some of the existing experimental observations, which are not fully understood in detail.

In this letter, we present density functional theory (DFT) calculations of the interface between P3HT and semiconducting/metallic CNTs in order to assess the feasibility of such a PV heterojunction design by understanding different roles played by the semiconducting and metallic tubes. Our results demonstrate that the semiconducting tube could form an ideal type-II heterojunction with negligible charge transfer at the interface and thus may be a suitable replacement for the fullerenes in these excitonic solar cells. In the case of the metallic tube, however, our calculations indicate a sizable charge transfer in the ground state as a result of chemical potential equilibration. The resulting built-in potential is found to be quite small and without the formation of interface states.

All electronic and structural properties of the systems considered in this work were obtained using DFT, employing a nonempirical gradient-corrected exchange-correlation functional.[22] Ultrasoft psuedopotentials[23] are used to describe the core electrons, and the wave functions and charge density are expanded in plane waves with kinetic energy up to 25 and 160 Rydberg, respectively, to obtain converged values.

For P3HT, the highest occupied molecular orbital (HOMO) and lowest unoccupied molecular orbital (LUMO) are π and π^* in character, respectively. The calculated HOMO–LUMO gap of 1.15 eV from the Kohn–Sham (KS) single particle states is substantially lower than the experimental band gap ($\sim$1.9 eV), as is generally observed in the DFT-KS approach. Introducing a second P3HT chain parallel to the first reduces the gap by less than 0.1 eV in our calculations. For the CNT, (10,2) and (12,3) tubes are used to represent typical $\sim$1 nm semiconducting and metallic CNTs, respectively. In the combined CNT/P3HT system, more than 1300 valence electrons are treated in the simulation cell with periodic boundary conditions. For the semiconducting tube, two different orientations were assessed by having the CNT placed parallel (*P*) and orthogonal (*O*) to the P3HT (see Figure 1) in order to test whether a qualitative difference exists when the interaction is varied. The simulation cell contains six thiophene units of the regioregular P3HT and a single chiral turn of the (10,2) CNT, measuring 23.9 Å in its axial direction. Upon relaxation, a minor axial strain is induced on the P3HT by the CNT; however, this strain has almost no impact on the electronic structure.[24] The interaction with the (12,3) metallic tube is studied only in the orthogonal (*O*) configuration with a single chiral turn, measuring 19.7 Å in the axial direction. A single **k**-point in the Brillouin zone (BZ) at Γ was used to describe the electronic structure for the semiconducting tube, while for the case of the metallic tube, two Monkhorst−Pack **k**-points (including $\mathbf{k} = 0$)[25] were used along the axial direction, together with Fermi−Dirac smearing at 300 K. All P3HT/CNT systems were fully relaxed with all atomic forces smaller than 0.01 eV/Å. Key properties calculated for separated and interface systems are summarized in Tables 1 and 2, respectively.

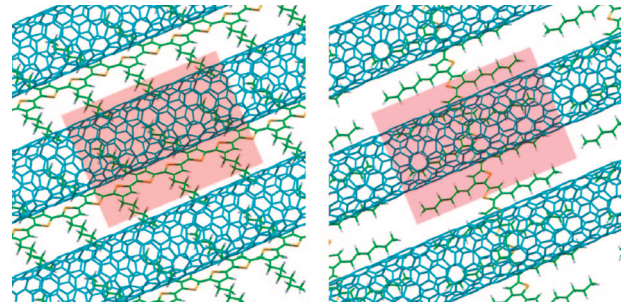

Figure 1. Heterojunction interface model used in calculations. (left) P3HT/CNT(10,2) in *P* configuration. (right) P3HT/CNT(10,2) in *O* configuration. The red shaded area represents the periodically repeating simulation super cell used in the calculations.

Table 1. Work function and KS energy gap (in eV) of individual P3HT, semiconducting CNT(10,2), and metallic CNT(12,3)

	P3HT	CNT(10,2)	CNT(12,3)
W_f	−4.0	−4.7	−4.3
KS gap	1.10	0.88	N/A

Table 2. Energetic parameters (in eV) of the interfaced P3HT/CNT heterojunctions for the semiconducting (10,2) and metallic (12,3) tubes[a]

	CNT(10,2)-*P*	CNT(10,2)-*O*	CNT(12,3)
LUMO offset	0.82	0.90	1.00
HOMO offset	0.60	0.67	0.06
KS gap	0.28	0.19	N/A

[a] LUMO (HOMO) offsets refer to the energy differences between the effective P3HT LUMO (HOMO) and CNT(10,2) LUMO (HOMO) for the semiconducting tube, while it refers to the effective P3HT LUMO (HOMO) energies with respect to the Fermi energy in the case of the metallic tube.

The interaction energy between P3HT and the semiconducting CNT was determined to be 0.13 and 0.01 eV (per simulation cell) for the *P* and *O* configurations, respectively. This difference stems from the difference in the contact area between the two, as expected. To assess the extent of the charge transfer, we compared the total charge density projected onto that of atomic orbitals, which unambiguously belong to either P3HT or CNT atoms. The projected density of states (DOS) on atom *I* was obtained using

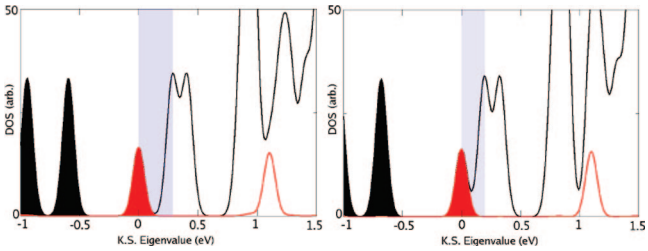

Figure 2. Density of states (DOS) in the vicinity of Fermi level for P3HT/CNT(10,2) in *P* configuration (left) and in *O* configuration (right). Projected DOS stemming from the P3HT is shown in red. The blue shaded areas represent the KS energy gap. Occupied states are shown filled while unoccupied states are shown empty. Gaussian broadening with 0.1 eV is used.

$$P_I(E) = \int_{\mathrm{BZ}} \mathrm{d}k\omega(k) \sum_i \sum_l \left| \langle \varphi_{I,l} | \psi_{i,k} \rangle \right|^2 \delta(E - \epsilon_{i,k})$$

where $\varphi_{I,l}$ are the orthonormalized (valence-pseudo) atomic orbitals for atom I and $\omega(k)$ is the weight in BZ integration and $\Psi_{I,k}$ and $\epsilon_{i,k}$ are Kohn–Sham wave functions and eigenvalues, respectively. Lowdin charges are then calculated by integrating the projected density over energy E multiplied by the corresponding electron occupation. The extent of charge transfer is then quantified by comparing the Lowdin charge of the combined systems and of the noninteracting separated P3HT and CNT. For both the *P* and *O* orientations, no sizable charge depletion for the P3HT sulfur atoms is observed, in contrast to what has been suggested in recent experiment[16] for the case of semiconducting CNT. Rather, our calculations show negligible charge transfer from P3HT to the semiconducting CNT, with <0.02 *electron* for both *P* and *O* configurations.

The HOMO/LUMO levels of a *single strand* of P3HT and the (10,2) CNT were calculated to be $-4.0/-2.8$ eV and $-4.7/-3.8$ eV from the local vacuum level, respectively (Table 1). Assuming that the surface polarization is negligible (therefore the local vacuum level and that at an infinite distance are approximately the same),[26] the interface of these two systems is expected to form a type-II heterojunction if the interaction does not result in a significant charge redistribution. One would expect this to be the case based on the negligible charge transfer observed in our calculations. Figure 2 shows the density of states (DOS) near the Fermi level for the interface in both *P* and *O* configurations. The projected DOS on the P3HT (red curve) shows the effective HOMO π and LUMO π^* states of the conjugated polymer. While the effective P3HT HOMO state fully accounts for the topmost occupied KS state of the interface system, the effective P3HT LUMO state has a non-negligible mixing with the CNT conduction band states. Therefore the corresponding unoccupied KS state of the combined system is about 95% and 80% P3HT in character for *P* and *O* configurations, respectively. This is not a surprising observation, given that the P3HT LUMO state is positioned energetically well inside the CNT conduction band and at the same time spatially in very close proximity to the CNT sidewall (~0.4 Å).

The DOS clearly shows the formation of type-II energy alignment at the heterojunction interface. The blue shaded region in Figure 2 indicates the KS energy gap of the combined

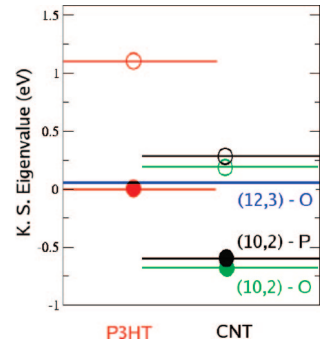

Figure 3. Energy alignments of effective P3HT and CNT HOMO/LUMO levels for the P3HT/CNT(10,2) heterojunction in parallel (black) and orthogonal (green) configurations. For the P3HT/CNT(12,3) heterojunction, alignment is with respect to the Fermi level (blue). The eigenvalue of the effective P3HT HOMO state is taken as the reference energy (0 eV). The difference of the effective P3HT energy gap for different interfaces is almost indistinguishable at this scale and neglected for clarity in the figure.

interface system. Effective HOMO/LUMO alignments of the P3HT and CNT at this interface are schematically shown in Figure 3, where the P3HT (CNT) levels are shifted to the left (right) horizontally. The alignments are altered by only ~0.1 eV at the interface with respect to the alignments that would be expected from the separated noninteracting P3HT and CNT components. This result may be useful for experiments because it demonstrates that a type-II heterojunction formation can be readily expected by simply, in principle, choosing an appropriate semiconducting CNT.

This observation, however, does not hold in the case of the metallic CNT. For the metallic CNT, we consider the (12,3) CNT only in the orthogonal (*O*) configuration, as mentioned earlier. Here, we predict a significant charge transfer of almost 0.3 *electron* to the CNT, indicating that there is a substantial interaction between the metallic (12,3) CNT and P3HT at the interface. The interaction energy was calculated to be 0.20 eV (per simulation cell). Figure 3 (left inset) shows the change in the electronic charge for different atomic species upon interface formation. As can be seen in this figure, there is charge accumulation for the CNT while the charges are depleted substantially from the P3HT sulfur atoms as suggested previously.[16] The calculated work function of the isolated (12,3) tube is -4.3 eV, approximately 0.3 eV lower in energy than the HOMO level calculated for the isolated P3HT strand (Table 1). When the interface is formed between the two, the Fermi level lies 0.06 eV above the effective P3HT HOMO level, as seen from the PDOS (Figure 4), due to the charge transfer to the CNT. The alignment of the effective P3HT HOMO state and the Fermi level of the system is not coincidental but rather the result of the chemical potential equilibration between the P3HT and metallic CNT. Although one might have expected the formation of interface electronic states, which would result in Fermi level pinning of this CNT within the P3HT gap, our results do not show such electronic states.

It is of interest to discuss these results in the context of photovoltaic cells, where the question of whether a metallic CNT could be employed in an efficient device remains open.

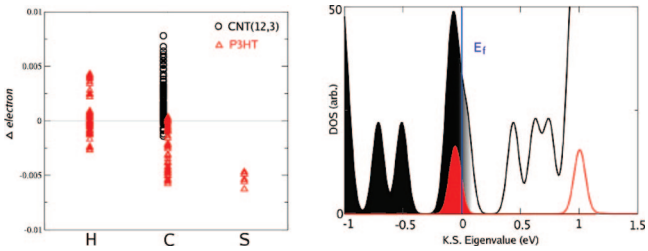

Figure 4. Electron density change for constituting atoms in case of P3HT/CNT(12,3) where significant ground-state charge transfer in observed at the interface (left). Density of states in the vicinity of Fermi level for P3HT/CNT(12,3) in *O* configuration (right). Projected DOS stemming from the P3HT is shown in red. The blue vertical line represents the Fermi level. Occupied states are shown filled while unoccupied states are shown empty. Gaussian broadening with 0.1 eV is used.

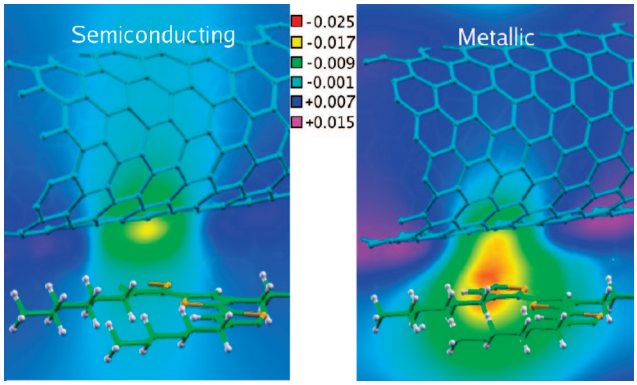

Figure 5. Induced change in the electrostatic potential (in atomic units) by the interface formation, $\Delta V(r) = V(r) - V_{CNT}(r) - V_{P3HT}(r)$, at the fixed ionic positions near the interface for the semiconducting (10,2) CNT case (left) and metallic (12,3) CNT case (right) in *O* configuration. The cutting contour plane approximately bisects the CNT diameter including the point of the most negative potential change.

On the one hand, once an exciton in the P3HT phase diffuses to the heterojunction interface with the metallic tube, it could undergo enhanced recombination within the tube due to the lack of an electronic band gap.[15] On the other hand, a different possibility would be for the exciton to undergo electron transfer first, leaving the hole behind. This exciton dissociation step would then need to be followed by charge separation away from the interface in order to observe photocurrent.

For this latter possibility, we compute changes in the electrostatic potential profile due to the interface formation between P3HT and CNTs in order to understand how the presence of CNTs would affect *locally* the additional charges on P3HT. Figure 5 shows the potential near the interface, subtracted by that of the individual P3HT and CNT components, for both the metallic and semiconducting CNT cases. Contrary to the case of a semiconducting tube where a shallow potential drop occurs near the CNT, a strong potential drop was observed *on* the P3HT for the metallic tube case. The presence of the metallic CNT induces this attractive region for negative charges on the P3HT. In a conventional approximation, where the creation of a single exciton is assumed not to alter qualitatively the potential profile, the interfaced P3HT attracts the electron rather than the hole. In the context of the exciton dissociation step of the excitonic PV mechanism,[4] this acts unfavorably against the desirable electron transfer to the metallic CNT from P3HT.

Furthermore, even if such an electron transfer across the heterojunction were to occur, our calculations suggest that the electron and hole may not be efficiently separated from the interface region. It has been proposed[17] that the built-in potential might then play a key role in drifting the hole away from the interface, inhibiting charge recombination across the interface. In the context of this junction-induced charge-separation model, our calculated built-in potential amounts only to 0.06 eV for the case considered here. Although an accurate estimate of the exciton binding energy across the interface is unavailable, this potential is likely to be quite small compared to the binding energy, therefore making charge separation highly unlikely at the metallic CNT/P3HT interface.

In summary, we have investigated the heterojunction interface between P3HT and CNT in the context of PV cells using quantum mechanical ab initio calculations. For the semiconducting (10,2) CNT, our results show that there is a rather small interaction between the CNT and the polymer, resulting in a type-II heterojunction, essentially as might be predicted from the isolated properties of the two. However, in the case of the metallic (12,3) CNT tube, we find a significant amount of charge transfer from P3HT to the CNT in the ground state, making P3HT strongly more attractive for the negative charges at the interface. Therefore, the electron transfer to the CNT could be unfavorable in the exciton dissociation step. Our results furthermore do not show any formation of interface electronic states that could pin the CNT Fermi level within the P3HT gap. The built-in field of the heterojunction was therefore found to be quite small (0.06 eV), unlikely to contribute significantly to the subsequent charge separation at this interface.

When a mixed distribution of semiconducting and metallic tubes are present, as in experiments, it is likely that the metallic tubes interact more strongly with P3HT because of the stronger electrostatic interaction due to the charge transfer. This is also reflected in our calculated interaction energies in the *O* configuration: 0.01 and 0.20 eV for the semiconducting (10,2) CNT and metallic (12,3) CNT, respectively. This could result in a majority of the interfaces being inefficient PV heterojunctions with the metallic tube for which the P3HT excitons are unlikely to undergo the charge separation. Although there exists a possibility for CNT defects to give rise to interface state formation,[16] such rather rare phenomena are unlikely to lead to a large photocurrent. The very small photocurrent observed for the P3HT/CNT in ref 16 (in $\sim\mu$A/cm^2 range), compared to other P3HT/fullerene or P3OT/CNT heterojunctions, may not be surprising in light of our present theoretical results.

Acknowledgment. This work was performed under the auspices of the National Science Foundation by the University of California Berkeley under grant no. 0425914, and by funding from the Industrial Technology Research Institute. Computations were performed at the National Energy Research Scientific Computing Center. The Quantum-Espresso code (www.quantum-espresso.org) was used for calculations.

References

(1) Huynh, W.; Dittmer, J. J.; Alivisatos, A. P. *Science* **2002**, *295*, 2425.
(2) Brabec, C. J.; Sariciftci, N. S.; Hummelen, J. C. *Adv. Funct. Mater.* **2001**, *11*, 15.
(3) Coakley, K. M.; Liu, Y.; Chiatzun, G.; McGehee, M. D *MRS Bull.* **2005**, *30*, 37.
(4) Forrest, S. R. *MRS Bull.* **2005**, *30*, 28.
(5) Gledhill, S. E.; Scott, B.; Gregg, B. A. *J. Mater. Res.* **2005**, *20*, 3167.
(6) Ma, W.; Yang, C.; Gong, X.; Lee, K.; Heeger, A. J. *Adv. Funct. Mater.* **2005**, *15*, 1617.
(7) Coakley, K. M.; McGehee, M. D. *Chem. Mater.* **2004**, *16*, 4533.
(8) Padinger, F.; Rittberger, R. S.; Sariciftci, N. S. *Adv. Funct. Mater.* **2003**, *13*, 85.
(9) Sariciftci, N. S.; Smilowitz, L.; Heeger, A. J.; Wudl, F. *Science* **1992**, *258*, 1474.
(10) Kanai, Y.; Grossman, J. C. *Nano. Lett.* **2007**, *7*, 1967.
(11) For a recent review, see, e.g., Hoppe, H.; Sariciftci, N. A. *J. Mater. Chem* **2006**, *16*, 45.
(12) Kymakis, E.; Alexandrou, I.; Amaratunga, G. A. J. *J. Appl. Phys.* **2003**, *93*, 1764.
(13) (a) Durrant, J. R.; Haque, S. A.; Palomares, E *Chem. Commun.* **2006**, 3279. (b) Asbury, J. B.; Hao, E; Wang, Y.; Ghosh, H. N.; Lian, T. *J. Phys. Chem. B* **2001**, *105*, 4545. (c) Grätzel, M. *Inorg. Chem.* **2005**, *44*, 6841.
(14) Kymakis, E.; Amaratunga, G. A. J. *Rev. Adv. Mater. Sci.* **2005**, *10*, 300.
(15) Kymakis, E.; Koudoumas, E.; Franghiadakis, I.; Amaratunga, G. A. J. *J. Phys. D: Appl. Phys.* **2006**, *39*, 1058.
(16) Geng, J.; Zeng, T. *J. Am. Chem. Soc.* **2006**, *128*, 16827.
(17) Kymakis, E. ; Amaratunga A. J. In *Organic Photovoltaics*; Sun, S-S., Sariciftci N. S. , Eds.; CRC Press: Boca Raton, FL, 2005.
(18) Ago, H.; Petrisch, L; Shaffer, M. S. P.; Windle, A. H.; Friend, R. H. *Adv. Mater.* **1999**, *11*, 1281.
(19) Kymakis, E.; Amaratunga, G. A. J. *Appl. Phys. Lett.* **2002**, *80*, 112.
(20) Kymakis, E.; Alexandrou, I.; Amaratunga, G. A. J. *Synth. Met.* **2002**, *127*, 59.
(21) Kymakis, E.; Amaratunga, G. A. J. *Sol. Energy Mater. Sol. Cells* **2003**, *80*, 465.
(22) Perdew, J.; Burke, K.; Ernzerhof, M. *Phys. Rev. Lett.* **1996**, *77*, 3865.
(23) Vanderbilt, D. *Phys. Rev. B* **1990**, *41*, 7892.
(24) Each thiophene unit is stretched by 0.02 Å compared to the isolated equilibrium P3HT geometry. This negligibly affects the P3HT electronic structure, for example, reducing the KS−DFT gap by only <0.05 eV.
(25) Monkhorst, H. J.; Pack, J. D. *Phys. Rev. B* **1976**, *13*, 5188.
(26) For a concise discussion of the difference, see, e.g., Cahen, D.; Kahn, A *Adv. Mater.* **2003**, *15*, 271.

NL0732777